The Pennsylvania State University
The Graduate School
Department of Civil and Environmental Engineering

REDUCING NITROGEN CROSSOVER IN MICROBIAL REVERSE-ELECTRODIALYSIS FUEL CELLS BY USING ION EXCHANGE RESIN

A Thesis in

Environmental Engineering

by

Maxwell J. Wallack

Submitted in Partial Fulfillment

of the Requirements

for the Degree of

Master of Science

May 2015

The thesis of Maxwell J. Wallack was reviewed and approved* by the following:

Bruce E. Logan
Kappe Professor of Environmental Engineering
Thesis Advisor

Michael A. Hickner
Associate Professor of Materials Science and Engineering

Manish Kumar
Assistant Professor of Chemical Engineering

Peggy A. Johnson
Professor of Civil Engineering
Head of the Department of Civil and Environmental Engineering

*Signatures are on file in the Graduate School

ABSTRACT

Reverse electrodialysis (RED) is a technology that uses high and low concentration salt solutions between a stack of alternating anion and cation exchange membranes to induce an electrical current. A RED stack installed between the anode and cathode of a microbial fuel cell (MFC) is called a microbial reverse electrodialysis cell (MREC). An MREC produces a greater power density than an MFC alone. When a RED stack is powered using ammonium bicarbonate salt solutions, nitrogen in the form of negatively-charged carbamate can be transferred through an anion exchange membrane (AEM) into the anode chamber. The loss of this nitrogen into the anode chamber is not sustainable or economical. Total ammonia nitrogen (TAN) concentrations in the anode chamber >500 mg/L can also prevent bacteria from efficiently utilizing acetate, reducing power production by the cell.

To reduce nitrogen crossover into the anode chamber, an additional low concentration (LC) chamber and AEM were installed between the high concentration cell in the RED stack and the adjacent anode chamber, and ion exchange resin was added to increase the chamber conductivity and reduce internal resistance. With this configuration, the overall nitrogen crossover into the anode was reduced by up to 96.5% compared to a standard configuration (no additional chamber) in a 24-hour fed-batch cycle. Anode pH rose from 8.5 to 10.5, instead of decreasing as is normally observed in an MREC. Resistance due to all membranes in the stack increased from 103 Ω-cm^2 to 295 Ω-cm^2, and an additional 637 Ω-cm^2 resistance was introduced by the solution in the low concentration chamber. When the additional LC chamber was filled (50%) with anion exchange resin, solution resistance decreased by 74% to 166 Ω-cm^2. In a lab-scale MREC, it was estimated that three additional RED cell pairs would be necessary to make up for power loss due to the membrane and solution resistance introduced by the LC chamber.

TABLE OF CONTENTS

LIST OF FIGURES

LIST OF TABLES

ACKNOWLEDGEMENTS

I would like to thank my adviser Dr. Bruce Logan for giving me the opportunity to work on microbial fuel cells, for help working through some of the difficult problems I encountered, and the generous time spent editing my thesis. It has been a powerful learning experience. In addition to Dr. Logan, I would like to thank my committee advisers Dr. Michael Hickner and Dr. Manish Kumar for their input and time spent reading and editing my thesis.

My membrane work would not have been possible without input from Dr. Hickner and Dr. Geoffery Geise, who assisted my understanding of ion exchange membranes and evaluated many of the tests I performed with membranes and ion exchange resin. I would also like to extend thanks to Dr. Marta Hatzell, for introducing the concepts of microbial reverse electrodialysis cells to me, and for her constant availability to troubleshoot.

Finally, I would like to thank the King Abdullah University of Science and Technology and Air Products for their financial support of my project.

Chapter 1

Introduction

In the year 2013, the world population was approximately 7.2 billion [1]. A significant amount of energy was used to sustain that number of people: 529 quadrillion BTU (quads) of energy was used worldwide in 2012 [2]. In the United States alone, 97.4 quads was used in 2013, of which 38.2 quads was for electricity generation [3]. The majority of energy production in the US was derived from coal, natural gas, and nuclear power (in that order). Coal and natural gas produce a significant amount of CO_2 when combusted. Coal can produce up to 229 pounds of CO_2 for every million BTU of energy [4]. According to the most recent IPCC report, rising CO_2 levels caused by this type of anthropogenic activity will account for an estimated increase of 0.3-0.7 °C in the atmosphere by the year 2035 [5]. By 2100, global mean temperature could rise by 4.8 °C. This change, compounded with other environmental factors, could have severe effects in the next one hundred years on human health, ocean levels, and agriculture. Reducing CO_2 emissions is imperative to avoid additional impacts on global temperatures [5].

One way to reduce emissions from fossil fuels is to use less energy. Wastewater treatment plant (WWTP) facilities in the United States comprise 4% of the energy footprint [6] . Energy consumption can be reduced at WWTPs by implementing alternative designs to the conventional WWTP system, which typically consists of a clarifier, an activated sludge aeration tank and clarifier, and additional nutrient removal systems. Microbial fuel cells (MFCs) have emerged as a potential alternative to biological treatment systems of the WWTP process, such as activated sludge [7, 8]. In an MFC, organics and nutrients in the wastewater stream are consumed by bacteria and removed, resulting in partially treated water. These bacteria generate electrons that flow through an external circuit, so electrical energy can be captured. If

implemented correctly, an MFC could be used to treat wastewater and generate enough power for the WWTP to operate as energy neutral.

The power produced by an MFC is an important trait for measuring its performance. The power densities produced by cube MFCs fed 1 g/L sodium acetate (NaAc) and 50 mM PBS are around 1.1 W/m^2 when normalized by the projected surface area of the cathode [9]. One way of increasing power densities is to use a reverse electrodialysis (RED) stack in an MFC, a configuration that is referred to as a microbial reverse-electrodialysis cell (MREC). A RED stack consists of alternating cells of high and low concentration salt solutions, each encompassed by alternating positively and negatively charged ion exchange membranes. Positively charged salt ions are transported from high concentration (HC) solution to low concentration (LC) solution through the cation exchange membrane (CEM), while negatively charged salt ions are transported from the HC solution to LC solution through the anion exchange membrane (AEM). This ion transport induces positive ion flow in one direction and negative ion flow in the other, which establishes a current. Typically, the RED stack is separated from the anode and cathode chambers in an MREC by AEMs, to enable higher power generation.

Solutions in the RED stack are contained in closed-loop systems. Sea and river waters, which can be found together at river and ocean boundaries, can be used as the HC and LC salt solutions. Utilizing solutions like ammonium bicarbonate (AmB), instead of sodium chloride, allow for higher potential energy because the salt concentrations can be controlled. Additionally, thermolytic AmB solutions can be distilled with low-grade waste heat to their original high and low concentrations, preserving the concentration gradient necessary for maximum power [10, 11]. An MREC powered by AmB and fed 1 g/L NaAc was shown to increase the power density

of an MFC from 1.1 W/m^2 to 5.4 W/m^2 when normalized by the projected surface area of the cathode [10].

One problem associated with using AmB in an MREC is that some of the nitrogen is present in the form of negatively-charged carbamate ($NH_2CO_2^-$). Carbamate can pass from high concentration solution through the AEM, and into the anode chamber [10]. Loss of nitrogen from the RED stack is uneconomical for long-term use, and wastewater cannot be discharged if nitrogen concentrations are too high. Additionally, total ammonia nitrogen (TAN) concentrations above 500 mg/L in the anode chamber inhibit acetate uptake by the exoelectrogenic bacteria [12]. This inhibition can lower the overall power density of the system. In one test, an MREC using AmB in the RED stack had 590 mg/L TAN in the anode chamber after 24 h [10]. There is only one previous report on a method to reduce nitrogen crossover. Luo et al. [13] introduced an additional RED cell using a CEM between the stack and the anode to mitigate nitrogen crossover. This configuration resulted in a reduction in nitrogen crossover by 60% to 311 mg/L TAN, and energy recovery via hydrogen production was not affected [13]. However, this amount of TAN crossover is still too high to make the process useful for power generation and wastewater treatment.

1.1 Objective

The objective of this work was to reduce the quantity of nitrogen that is transferred into the anode chamber of an MREC powered by ammonium bicarbonate solutions. It was hypothesized here that an additional LC cell and AEM (as opposed to CEM) would reduce nitrogen crossover into the anode, and that the increased resistance produced by using this configuration could be decreased by using ion exchange resin as a conductive material in the

additional cell. Ion exchange resins have been used in microbial desalination cells (MDCs) to improve solution conductivity, and therefore cell performance [14-18]. To test this hypothesis, different ion exchange resins and membrane setups were examined to identify the most conductive system. Then, nitrogen crossover in systems with and without an additional LC cell were measured for the amount of TAN present in the anode chamber after 24 h. Finally, the additional resistance was examined in these systems in the presence and absence of ion exchange resin.

Chapter 2

Literature Review

2.1 Microbial Fuel Cell

A microbial fuel cell can be used to harvest energy from organic matter by using anaerobic, exoelectrogenic bacteria to produce electrons that can be transferred through an external circuit (Figure 2.1). Bacteria, such as various *Geobacter* species, consume a carbon source at the anode and produce electrons [8, 19]. These electrons flow through the external circuit to the cathode, where they are combined with oxygen to form water [20]. Thus, MFCs can be used to reduce the biochemical oxygen demand (BOD) of a wastewater, and uptake nutrients like nitrogen while simultaneously producing electricity.

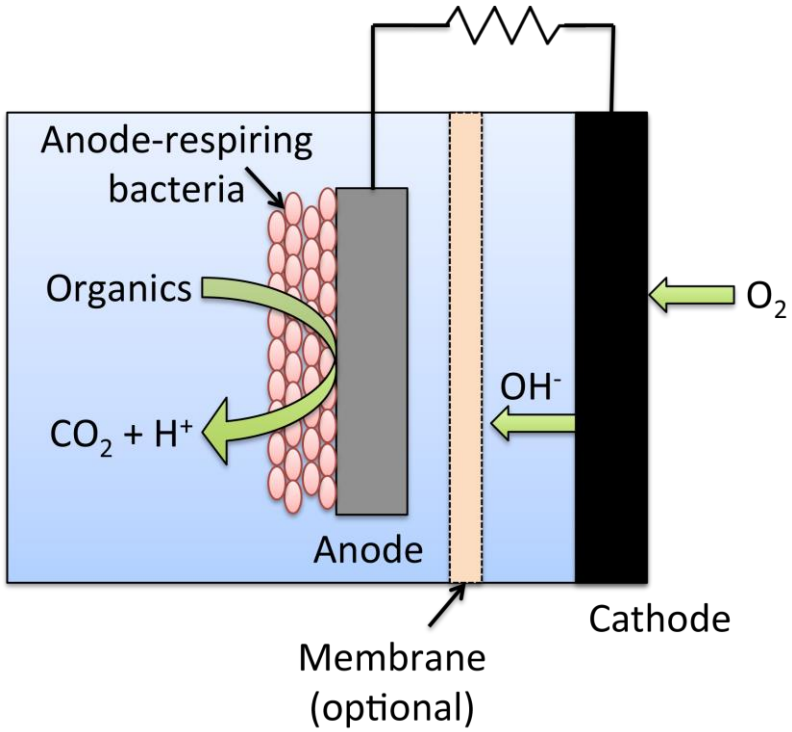

Figure 2.1: A microbial fuel cell. Exoelectrogenic bacteria respire organics, producing hydrogen and electrons. The electrons flow through the external circuit, where they can be converted to power. Oxygen passing through the cathode is re-combined with the hydrogen to form treated water. Taken from The Biodesign Institute at Arizona State University [21].

An MFC contains a brush anode and an air cathode that are electrically connected externally. Oxygen diffuses into the MFC through the air cathode, which is typically made using carbon cloth and a platinum catalyst [8]. A diffusion layer, such as multiple polytetrafluoroethylene (PTFE) layers, can be applied to the air-facing side of the cathode to prevent water from leaking out of the MFC while simultaneously allowing less oxygen transfer [8]. The use of a brush anode, which is constructed from graphite fibers, provides a high specific surface area for a large amount of bacteria [8].

The open circuit voltage (OCV) of an MFC can theoretically produce 1.1 V, with 0.6-0.8 V commonly produced in practice [8, 20]. An MFC with brush anode, air cathode, and 30 mL liquid volume fed with 1 g/L sodium acetate (NaAc) and 50 mM phosphate buffer solution (PBS) generally produces a power density of approximately 1100 mW/m^2 [9]. For the same conditions, except using 8 mM PBS to simulate the solution conductivity of a domestic wastewater, the MFC produced only 460 mW/m^2. Increasing power densities will help implementation of MFCs for wastewater treatment.

2.2 Reverse electrodialysis

Salinity gradient energy (SGE) can be used in conjunction with MFCs to increase net power produced from organic matter. SGE technologies rely on the energy difference between high and low concentration salt solutions. The energy available due to the concentration difference between river (0.015-1.5 mS/cm) and sea (~70 mS/cm) water is equivalent to a hydraulic head of 270 meters [22]. Sea and river water are useful solutions for SGE because they naturally occur together when rivers flow into oceans, but available land space near coastal regions and concentrated salt brines is limited. Additionally, the use of natural waters introduces microorganisms that can contribute to membrane fouling, which can decrease power and reduce

the operational lifetime of the system [23]. The two most common technologies to harness SGE are pressure-retarded osmosis (PRO) and RED [24]. In PRO, a water selective membrane is used to separate fresh water and salt water. Fresh water passes through the membrane to equilibrate the salt concentration difference and increases pressure on the salt water side. The increased water pressure can be used to drive a turbine.

In RED, ion selective membranes are used to generate an electrical current. Salt and other ions can pass from high concentration to low concentration solutions through ion exchange membranes of opposite charge. Anions in a salt pass through a positively-charged AEM, while CEMs would selectively allow cations to pass. By setting up a high concentration salt chamber flanked by two membranes and fresh water, salt ions are transported from the high concentration chamber into fresh water. When an AEM and CEM are used on either side, anions and cations travel in opposite directions to create a voltage difference. Due to the generation of a Donnan potential, ~0.16 V is produced per pair of Selemion (Asahi Glass, Japan) membranes with a 30 g/L NaCl high concentration solution and 1 g/L NaCl low concentration solution [25, 26]. A RED stack is created by using a series of alternating AEMs and CEMs with alternating high and low salt concentration cells (Figure 2.2).

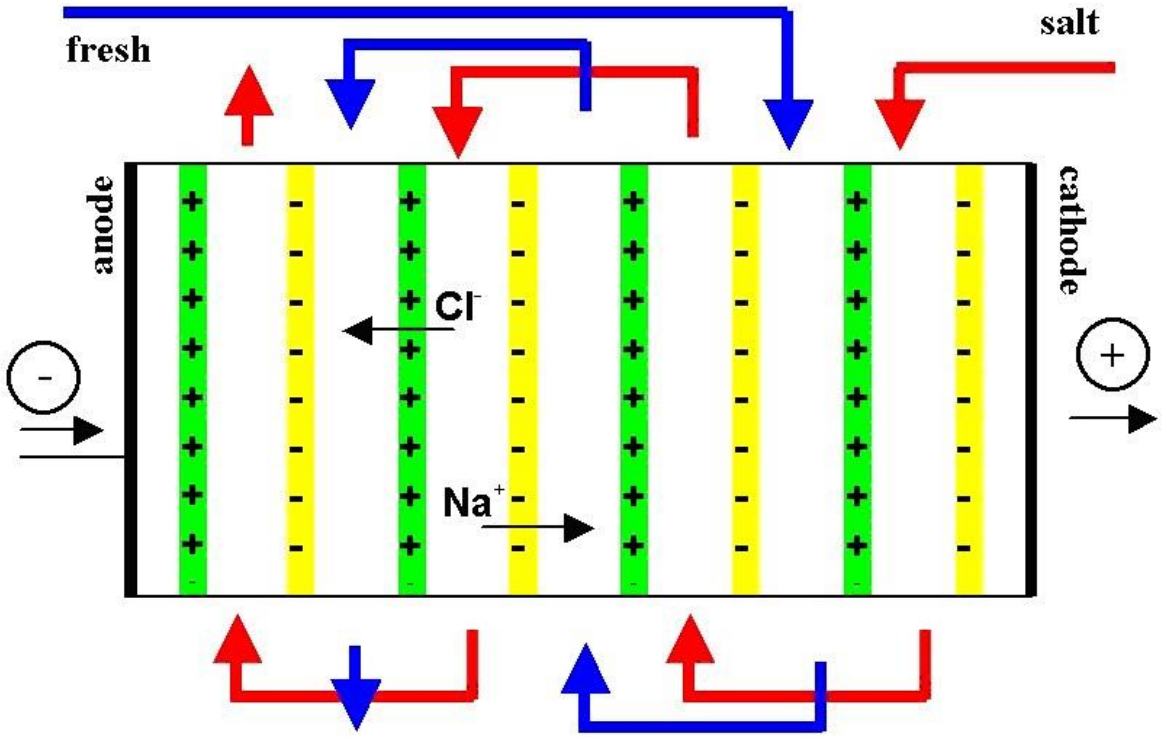

Figure 2.2: A reverse electrodialysis (RED) stack. Alternating membranes and HC and LC solutions creates an electrical gradient. The solution passes serially through the stack, though other cases can use single pass through each cell. Taken from ClimateTechWiki.org [27].

The gross power density (P_{net}) produced by a RED stack is a function of the potential (E_{OCV}) across the membranes, current density (j), number of membranes (N_m), ohmic resistance due to solution and membranes (R_{ohmic}), membrane concentration gradient resistance ($R_{\Delta C}$), membrane boundary layer resistance (R_{BL}), and pumping power (P_{pump}), and it is calculated as [28]:

$$P_{net} = \frac{E_{OCV} \cdot j - (R_{ohmic} + R_{\Delta C} + R_{BL}) \cdot j^2}{N_m} - P_{pump} \tag{2.1}$$

Increasing the number of paired membranes increases the stack voltage and power density, provided the voltage produced by membranes is greater than the resistance [29, 30]. Solution and membrane resistances ($R_{ohmic}, R_{\Delta C}, R_{BL}$) dictate power loss in the RED stack, with the low

concentration salt solution contributing the largest overall portion of the total stack resistance [31]. Spacers can be placed in between membranes to improve hydrodynamics and prevent the fluid from short-circuiting, and increase power. However, non-conductive spacers introduce what is known as the shadow effect, where ion transport through the membrane is blocked by the non-conductive spacer material. Conductive spacers help alleviate this problem by creating a path for ions to cross through both the spacer and membrane [32].

2.2.1 Membranes in RED

Membrane resistance is comprised of ohmic, boundary layer (along the membrane), and bulk concentration change (between solution and membrane) resistances [25, 28]. Faster flow of the salt solutions through the RED stack reduces both boundary layer and bulk concentration resistances [33]. The boundary layer is reduced by increased shear force on the membrane. Bulk concentration effects are minimized by replenishing solution in each cell more quickly to avoid large concentration gradients. However, increasing flow requires greater pumping energy and decreases the overall energy recovery efficiency in the system, so operational conditions must be balanced to maximize net power production.

Membranes with low resistance and high permselectivity are optimum for use in RED stacks. However, membranes with low resistance also usually have decreased permselectivity [34]. Membrane permselectivity dictates how well co-ions transfer through the membrane, and how well counter-ion transfer will be inhibited, according to the Donnan exclusion principle [26]. Permselectivity is determined by membrane construction and the solutions used [35]. A decreased resistance and high permselectivity must be balanced for optimum power production [36, 37]. Membranes have been custom-tailored for use in RED stacks with these properties in mind. Güler et al. [38, 39] developed very thin membranes with high ion exchange capacity to

reduce resistance, as reducing the membrane thickness reduced resistance in most cases. Profiled membranes, or patterned membranes, are physical modifications that integrate the function of a spacer by casting grooves throughout the membrane that channel the salt solutions to prevent short-circuiting. One test with membranes constructed with 200 μm wide, straight grooves showed a 10% increase in power due to the decrease in ohmic resistance, at the cost of increasing boundary layer resistance [40]. In another test, membranes were casted using a PTFE mold that created 300 μm diameter hemispherical protrusions. The altered flow path caused by the protrusions decreased ohmic, boundary layer, and diffusion boundary layer resistances, resulting in a 38% increase in power density compared to a system with non-patterned membranes and non-conductive spacers [41]. Profiled membranes also decrease pressure drop compared to systems with spacers, resulting in greater net power [33, 40].

2.2.2 Ammonium Bicarbonate

Using ammonium bicarbonate (NH_4HCO_3) in the RED stack, instead of other salt solutions like NaCl, has two advantages: solution regeneration can be accomplished using waste heat, and the salinity gradient can be controlled. As salt solutions are used in a RED stack, the HC solution loses ions and the LC solution gains ions, decreasing the salinity gradient. AmB is a thermolytic solution, meaning it is possible to distill it out of water using low-grade heat (40°C), making it possible to use waste heat to create salinity gradients for electricity production [11]. AmB can be condensed, allowing the regeneration of the HC and LC solutions [10, 42]. By controlling the salinity ratio, AmB can be used to generate solutions with an energy potential equivalent to 370 meters of head [10]. One disadvantage of using AmB is that bubbles can spontaneously form and accumulate in the RED stack. The bubbles reduce the available

membrane area for ion exchange, reducing total net power. The formation and retention of bubbles can be partially addressed through flow field and gasket design [43].

2.3 Microbial Reverse Electrodialysis Cell

MFCs and RED were recently combined into a single system, called a microbial reverse electrodialysis cell (MREC) [44]. In this system, the anode and cathode of an MFC are separated by the RED stack. Electrons flow from the exoelectrogenic bacteria on the anode to the air cathode through an external circuit, and the RED stack increases the voltage and therefore the power generated compared to the MFC alone. The RED stack reduces anode overpotential, allowing higher current that can increase power densities up to 5.6 W/m^2 [10], significantly higher than a standard MFC [9]. An MREC performs best when the membranes adjacent to the anode and cathode chambers are both of the same ionic type (i.e. anionic). HC salt solutions are used as the catholyte to reduce resistance. The maximum amount of power is generated when a LC RED cell is adjacent to the cathode, which creates a large concentration gradient. An AEM is placed between the HC catholyte and LC RED cell to induce the desired flow of anions toward the anode chamber.

MRECs have been configured to produce electricity, gas, and other beneficial chemicals while treating wastewater. MRECs that produce gases are a modification of a microbial electrolysis cell (MEC). MECs are constructed similarly to MFCs, but a voltage is applied to increase the anode potential and induce hydrogen evolution. Instead of energy being recovered from electricity, it is recovered in the form of hydrogen gas (H_2). The RED stack in an MREC decreases the amount of applied voltage necessary for hydrogen evolution [45]. MRECs can be used for hydrogen and methane production [45-47]. In previous tests, hydrogen was produced

with no external energy sources [13, 45]. Energy obtained by producing hydrogen was 1.5× greater than energy recovery from electrical power production [48].

2.4 Nitrogen Crossover

When AmB is used in an MREC, nitrogen can cross over from the RED channel into the anode. Nitrogen crossover prevents the anolyte from being discharged safely, the loss of nitrogen is uneconomical, and high concentrations of ammonia can prevent acetate utilization by bacteria. Nitrogen crossover occurs because one of the chemical species present when AmB is dissolved in water, carbamate ($NH_2CO_2^-$), can cross through an AEM due to its negative charge [10]. Carbamate can account for 15% of the nitrogen in an AmB solution at pH 7 – 8.5 [49]. There is great potential for crossover because an HC AmB chamber is generally located directly adjacent to the anode chamber [10, 35]. TAN concentrations above 500 mg/L in a batch-fed MFC, and 3500 mg/L in a continuously-fed MFC, were found to inhibit acetate utilization by exoelectrogenic bacteria, reducing power production [12, 50].

Only one attempt has previously been made to reduce nitrogen crossover. Luo et al. [13] reduced nitrogen crossover in a hydrogen MREC by 60% when using an additional LC chamber and CEM adjacent to the anode. While gas generation and efficiency remained similar, 311 mg/L TAN was still present in the anolyte after one cycle, which greatly exceeds typical discharge requirements of nitrogen in wastewater (<5-10 mg-N/L).

2.5 Ion Exchange Resin

An additional LC chamber can be introduced between the anode and RED stack to reduce nitrogen crossover. Introducing an additional LC cell into the RED stack to reduce carbamate crossover, however, increases the internal resistance. Ion exchange resins can be used to increase

the conductivity of a solution, decreasing its resistance, if the resin has a relatively higher conductivity than the solution [51]. Ion exchange resins have not been previously studied to reduce nitrogen crossover in an MREC.

Ion exchange resins are available in a particle sizes ranging from 200-400 mesh (74-37 μm) to 20-25 mesh (841-707 μm) and larger. Most resins are made through the suspension polymerization method, where properties like high mesh (macroporous), gel resins, cross-linkage, and particle size are determined by altering the polymerization process [52]. The low degree of cross-linkage in gel resins is more beneficial for conductivity [53]. The ion exchange capacity (IEC) indicates the number of ions able to be absorbed by the resin. A larger capacity indicates an increased fixed ionic group concentration, which means the resin will be more conductive [53]. Other characteristics indicating high conductivity include smaller sized counter-ions, and resin in equilibrium with high concentration solution.

Microbial desalination cells have previously used ion exchange resin to decrease internal resistance [14-18]. MDCs utilize a desalination chamber instead of RED stack in between the anode and cathode. Salt water flows through the desalination chamber, and ions are driven through membranes on either side of the chamber due to the voltage difference between the anode and cathode. Instead of harvesting energy, desalinated water is produced. When ion exchange resin was added to the MDCs, ohmic resistance was reduced by 38-63% [14, 17, 18].

Chapter 3

Methods

3.1 Reactor Construction

A two-chamber (2C) reactor was constructed to determine solution and membrane resistances. The reactor was made by connecting in series six reactor sections, each a 4 cm acrylic cube drilled to contain a 3 cm diameter working chamber (Figure 3.1a). An AEM (Selemion AMV; Asahi Glass, Japan) or CEM (Selemion CMV; Asahi Glass, Japan) was installed halfway in the reactor between two gaskets to create a tight seal between the two equal-volume anode and cathode chambers. AEMs and CEMs were equilibrated in 1 M (HC) NaCl of 1.1 M AmB for at least 1 h and rinsed with deionized water (Synergy Ultra Water System; EMD Millipore) before installation in the reactor for their respective tests. Each chamber contained a platinum mesh electrode, inlet and outlet for solution, opening for an overhead stirrer (Petite Digital, 50-2500 RPM; Caframo, Ltd.), and a custom Teflon fitting close to the membrane to allow insertion of a Ag/AgCl reference electrode (RE-4B; Bioanalytical Systems, Inc.). The solutions were stirred at 800 RPM using an overhead stirrer. The platinum mesh and reference electrodes were connected to a potentiostat (Multi Potentiostat VMP3, Bio-Logic) for electrical measurements.

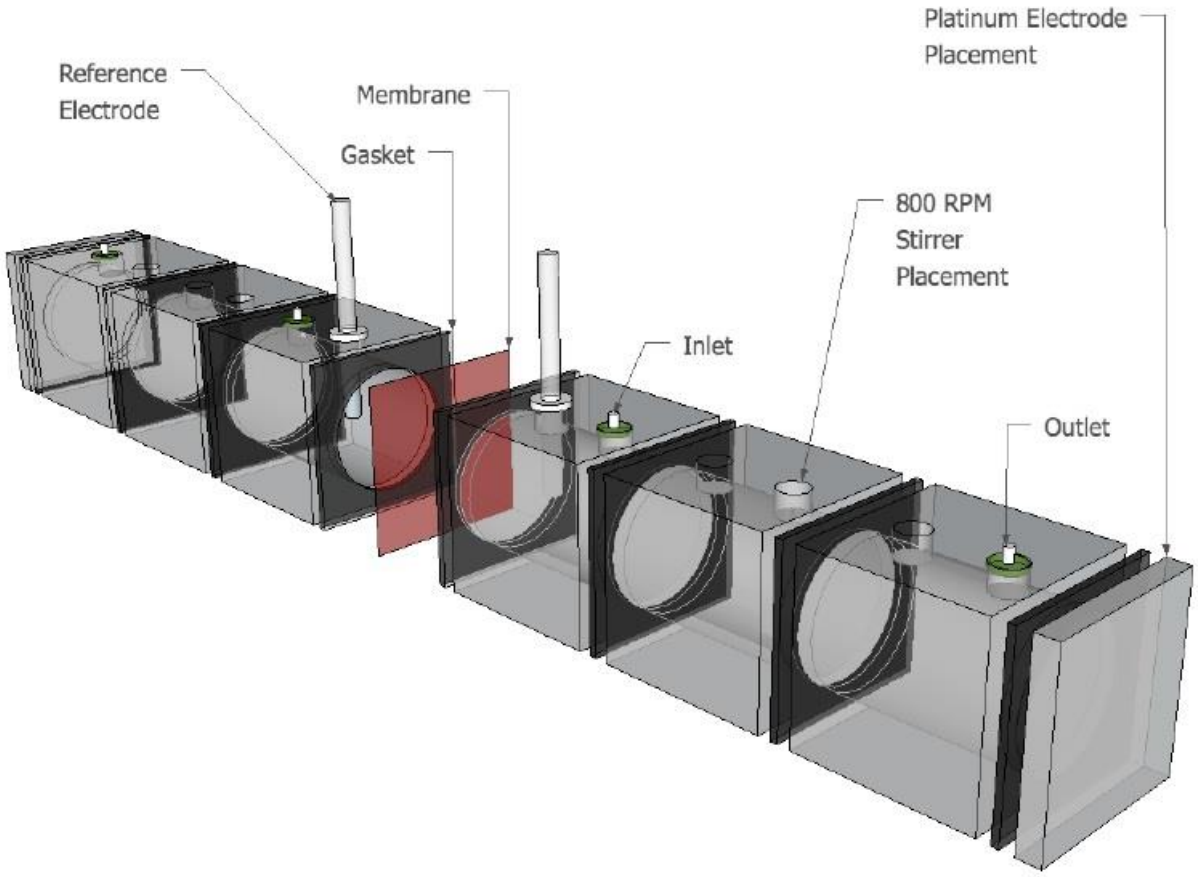
Platinum Electrode
Placement
Reference
Electrode
Membrane
Gasket
800 RPM
Stirrer
Placement
Inlet
Outlet

(A)

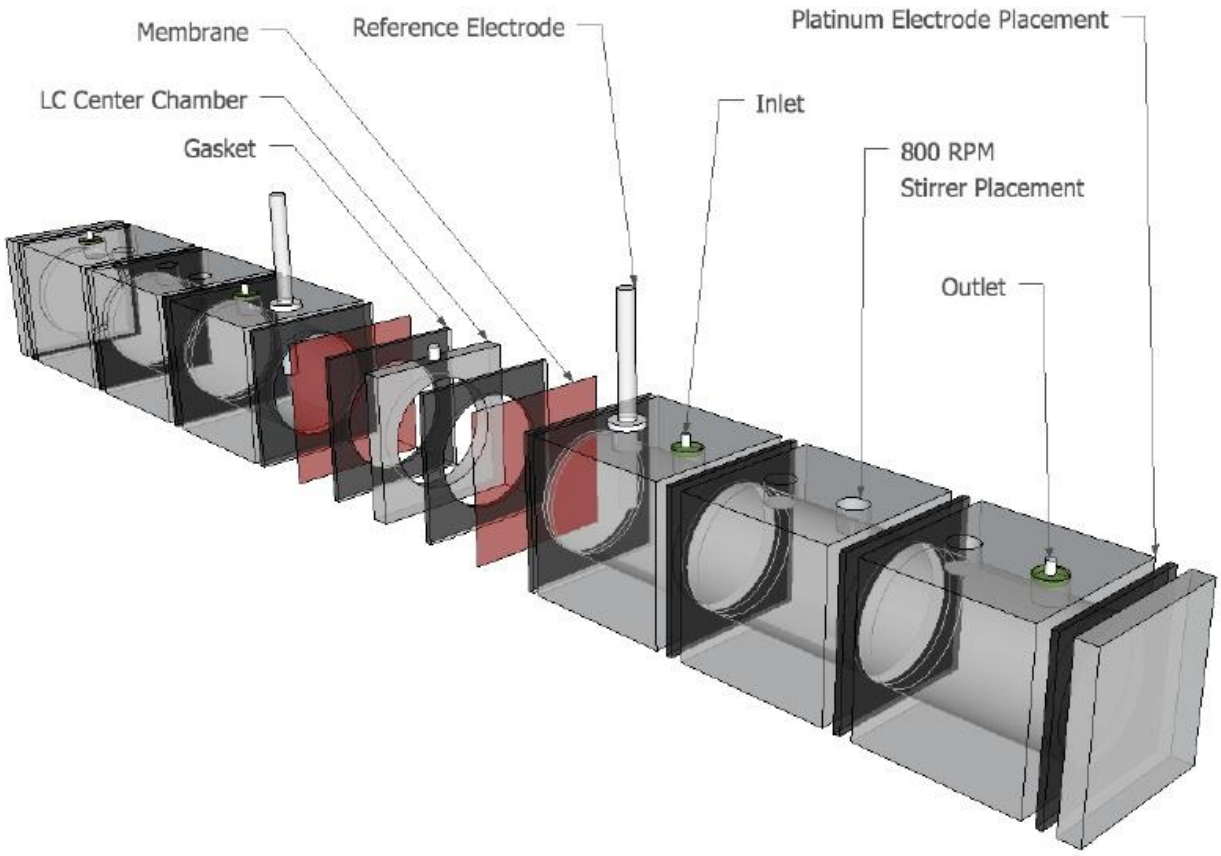

(B)

Figure 3.1: (a) The two-chamber (2C) reactor, built with 6 cube sections in succession. The reference electrodes are placed as close to the membrane as possible. (b) The three chamber (3C) reactor constructed from 6 cubes in succession and an additional thin center chamber that can contain resin. Two membranes are used in this system, on either side of the middle chamber.

A three-chamber (3C) reactor was constructed by adding an additional chamber and membrane to the 2C reactor to allow examination of the effect of ion exchange resin on the center chamber resistance. The center chamber had a width of 0.54 cm with a 3 cm diameter working area. Two membranes were used in this system, with each membrane placed on either side of the middle thin chamber (Figure 3.1b). Including the gaskets (0.158 cm each) used to seal the chamber, the total center chamber thickness was 0.856 cm. The other components and operation of the reactor was the same as described above for the 2C reactor. For resin

conductivity tests, 1-3 g (as indicated) of ion exchange resin was added to the center chamber. For all nitrogen crossover tests, only 3 g of ion exchange resin was tested in the center chamber. Resin mass was measured based on dry weight using a balance (PB303-S, Mettler Toledo). Ion exchange resin was equilibrated in 500 mL HC NaCl or HC AmB with stirrers for at least 8 h, rinsed with deionized water, and patted dry directly before installation between the two membranes in the center chamber for tests.

3.2 Testing Procedures

Membrane conductivity, ion exchange resin conductivity, and nitrogen crossover tests were performed to evaluate system performance. All tests were carried out in a temperature-controlled room (27.9 ± 0.6 °C). Solution conductivities (σ) were adjusted to room temperature using the linear coefficient for salt solutions provided by the manufacturer of the conductivity meter [54]. All reactors were equilibrated for 30 m in OCV before each test.

3.2.1 Membrane Resistance

A 2C reactor with an AEM membrane was used to measure baseline system resistance on a weekly basis prior to resin-based tests to ensure that the system resistance did not fluctuate over time (Table 3.1). HC solutions (1M NaCl, $\bar{\sigma} =$ 86.8 mS/cm at 25 °C) flowed in a single-pass through the anode and cathode chambers at 3 mL/min. The potentiostat was used to set the current between platinum mesh electrodes from 0 to 4 mA in 0.5 mA increments every 10 s. The voltage difference between reference electrodes was recorded for use in resistance calculations.

System baselines were also measured weekly using the 3C reactor. In addition to the same anolyte and catholyte conditions used for the 2C reactor, a HC NaCl solution flowed

single-pass upward through the center chamber at 2 mL/min. Potentiostat measurements were taken in the same manner as the 2C reactor.

Table 3.1: Reactor Setups and Programs for Background Measurements

Reactor Setup	Membranes	Test Use	BioLogic Program
HC | HC	AEM	Baseline	0-4 mA, 0.5 mA steps/10 s
HC | HC | HC	AEM	Baseline	0-4 mA, 0.5 mA steps/10 s
HC | LC | HC	AEM	Membrane resistance with dissimilar electrolytes.	0-4 mA, 0.5 mA steps/10 s
HC | LC | HC	CEM	Membrane resistance with dissimilar electrolytes. VMP3 program changed due to boundary conditions.	0-4 mA, 0.5 mA steps/2 s

High concentration (HC) and low concentration (LC) chambers in 2C and 3C reactors are separated by membranes (|).

The 3C reactor was also used to measure membrane resistances with dissimilar (HC and LC) electrolytes, to confirm performance consistent with previous measurements [55, 56]. Two membranes of the same type (AEM or CEM) were installed in the reactor. HC solutions (1 M NaCl) flowed in a single-pass through the anode and cathode chambers at 3 mL/min. LC solution (10 mM NaCl, $\bar{\sigma} = 1.07$ mS/cm at 25 °C) flowed in a single-pass upward through the center chamber at 2 mL/min. For AEM measurements, the potentiostat was operated at a stepped current between the platinum electrodes from 0 to 4 mA in 0.5 mA increments every 10 s. The voltage difference between the reference electrodes was measured for resistance calculations. For CEM measurements, the potentiostat was operated at a stepped current between the platinum electrodes from 0 to 4 mA in 0.5 mA increments every 2 s.

3.2.2 Ion Exchange Resin Conductivity

Two anion and cation exchange resins were tested for conductivity using the 3C reactor. Each type of resin was tested with a high and low IEC resin to determine conductivity differences (Table 3.2). The potentiostat was used to drive 0 to 4 mA of current through the platinum electrodes in 0.5 mA steps every 2 s. Anolyte and catholyte HC NaCl solutions both flowed single-pass at 3 mL/min. Single-pass LC NaCl flowed at 2 mL/min through the center chamber containing the resin.

Table 3.2: Ion Exchange Resin Qualities

Dowex Resin Name	Type	Abbreviation	Ion Exchange Capacity (meq/L)	Cross-Linkage (%)	Moisture Content (%)
1X2	Anion	AL	0.7	2	65-75
1X8	Anion	AH	1.2	8	43-48
50WX2	Cation	CL	0.6	2	74-82
50WX8	Cation	CH	1.7	8	50-58

Ion exchange capacity, cross-linkage, and moisture content data was gathered from Dowex technical bulletins [57]. The abbreviations indicate anion (A) or cation (C) exchange resin, as well as high IEC (H) or low IEC (L) properties.

Ion exchange resins were first tested using similarly-charged membranes in the reactor, as this was expected to be the most conductive configuration. The anionic (A), high IEC (H) resin Dowex 1X8 (AH) was tested in the 3C between two AEMs (Table 3.3). The cationic (C), high IEC resin Dowex 50WX8 (CH) was tested in the 3C between two CEMs. One, two, or three grams of resin was added to the reactor in each test. The anionic, low IEC (L) resin Dowex 1X2 (AL) was added between two AEMs (3 g) to test the difference between resins with different cross-linkage. The cationic, low IEC Dowex 50WX2 (CL) was also added between two CEMs (3 g) to test this difference with the cationic species. A mixed system containing 50% AH and 50%

CH resins by weight was tested in between one AEM and one CEM. One, two, or three grams of resin was added for each test.

Table 3.3: Membrane and Ion Exchange Resin Configurations for Resistance Tests

Membranes	Membrane Type	Dowex Resin	Resin Type	Mass Resin (g)
AEM-AEM	A	1X8	AH	1, 2, 3
AEM-AEM	A	1X2	AL	3
CEM-CEM	C	50WX8	CH	1, 2, 3
CEM-CEM	C	50WX2	CL	3
AEM-CEM	A and C	50% 1X8 50% 50WX8	AH and CH	1, 2, 3

The resin and membrane types indicate anion (A) or cation (C) exchange properties, as well as high IEC (H) or low IEC (L) resins.

3.2.3 Low Concentration Chamber Flow Rate

Further tests using two AEMs were conducted to understand resistance changes due to flow rate in the center chamber of the 3C reactor. The anode and cathode chambers were operated with HC (1 M NaCl) solutions running single-pass at 15 mL/min, and stirred at 800 RPM. LC solution (10 mM NaCl) flowed in a single-pass upward through the center chamber. Flow was controlled from 0.5 – 30 mL/min, corresponding to a hydraulic retention time (HRT) of 12 s – 12 m for a chamber volume of 6.2 mL. The potentiostat was operated at a stepped current between the platinum electrodes at 0.01, 0.1, 0.5, 1, 3, 7, and 10 mA for 2 seconds to test the maximum expected current range of the Selemion AMV [33]. Then, 3 g of Dowex 1X8 (AH) resin was added to fill the center chamber 50%. The same solution and potentiostat conditions were used, but flow through the center chamber was operated from 0.25 – 15 mL/min to have equivalent HRTs as the system without resin. The LC solution conductivity was measured at the

outlet in a second series of tests using flow rates of 2 – 8 mL/min to analyze the effect that a conductivity change had on the calculated membrane resistance.

3.2.4 Nitrogen Crossover

Nitrogen crossover was measured in a 2C reactor containing one AEM with solution conditions set to match the anode chamber and adjacent HC RED cell of an MREC. The anode chamber contained a buffer (B) of either 50 mM $NaHCO_3$ (pH = 8.5)[13] or 50 mM $NaHCO_3$-Na_2CO_3 (pH = 10.7) that was recycled at 15 mL/min using a 1 L storage reservoir. The cathode chamber contained HC solution (1.1 M NH_4HCO_3, $\bar{\sigma} = 80$ mS/cm) that was recycled at 15 mL/min using a storage reservoir (1 L). The initial solution conductivities and anolyte pH were measured at room temperature. Current (4 mA) was set between the platinum electrodes for 24 h to simulate a typical batch cycle in an MREC [10]. Nitrogen concentrations in the buffer were measured using standard methods [HACH Method 10031, High Range Test 'N Tube for Ammonia Nitrogen, and Orion 951007 Stock Ammonia Solution (1000 ± 5 mg/L) or HACH Ammonia-Nitrogen Standard Solution (1000 mg/L ± 5 mg/L)]. The standard additions method (sample spike) and standard solution method from HACH Method 10031 were performed to ensure accuracy. The final anolyte pH was measured at the end of every nitrogen crossover test.

Nitrogen crossover was also measured in a 3C reactor containing two AEMs to measure changes in TAN due to the use of an additional chamber which was filled with LC solution. Solution conductivity, anolyte pH, and TAN were measured as described for the 2C reactor. The anolyte was 50 mM $NaHCO_3$ buffer, and the catholyte was HC AmB. Both were recycled at 15 mL/min using 1 L reservoirs. LC AmB (11 mM, $\bar{\sigma} = 1.21$ mS/cm) flowed upward at 4 mL/min through the center chamber and was recycled in a 0.5 L reservoir. Following tests using an empty

chamber, 3 g of AH resin (50% chamber volume) was added to measure if there was additional reduction in nitrogen crossover. AmB was recycled at 2 mL/min through the center chamber to produce the same residence time used for the empty middle chamber. Current was set at 4 mA between the two platinum electrodes for 24 h, and the voltage difference between the reference electrodes was recorded using the potentiostat.

3.2.5 Ammonium Bicarbonate Chamber Resistance

Resistances were measured using the 2C and 3C reactors using AEMs to determine the additional resistance added by the center chamber. The 2C reactor was operated using 50 mM $NaHCO_3$ buffer (pH = 8.5) in the anode chamber, and HC AmB in the cathode chamber (B | HC). Both solutions flowed in a single-pass at 3 mL/min. The current was stepped between the platinum electrodes from 0 to 4 mA in 0.5 mA steps every 2 s. Voltage between the reference electrodes was recorded with the potentiostat. The 3C reactor tests were made using the same anolyte and catholyte conditions as the 2C reactor, and tested with the same electrochemical measurements. LC AmB was pumped through the center chamber at 2 mL/min (B | LC | HC). Measurements were made using either no resin or 3 g of AH resin in the middle chamber (B | LC + R | HC).

3.3 Reactor Resistance and Resin Conductivity Calculations

The total measured resistance between the reference electrodes (R_{meas}) for both the 2C and 3C reactors was calculated using Ohm's law as:

$$R_{meas} = \frac{\Delta U}{\Delta I} \tag{3.1}$$

where U is the voltage measured with a set current (I).

The volume of resin (V_{resin}) present in the center chamber was calculated as:

$$V_{resin} = \frac{m_{resin}}{\rho_{resin}}(1 + Sw)(1 - e) \tag{3.2}$$

where m_{resin} is the mass of resin added, ρ_{resin} is the moist density of the resin beads reported by the manufacturer (0.00161 lb/mL, Dowex 1; 0.00181 lb/mL, Dowex 50W), Sw = 0.2 is the increase in resin volume assuming a conservative resin swelling of 20% from values reported by the manufacturer, and e = 0.33 is the void space ratio estimated from the manufacturer void volume specifications (30-40%) for a low conductivity solution [57, 58]. The volume fraction of resin used in the center chamber was calculated as:

$$\emptyset_{resin} = \frac{V_{resin}}{V_C} \tag{3.3}$$

where V_C is the empty bed volume of the center chamber.

The solution resistances (R_{soln}) in the presence or absence of resin is calculated as:

$$R_{soln,i} = \frac{L_i}{A\ \sigma_{soln,i}\ (1 - \emptyset_{resin})} \tag{3.4}$$

where L_i is the characteristic length scale of the measurement, A is the cross-sectional area of the reactor (7.26 cm^2), and $\sigma_{soln,i}$ is the solution conductivity, where i indicates the anode chamber (An), center chamber (C), or cathode chamber (Cat). For the 2C and 3C reactors, the anode and cathode chambers had equal lengths where $L_{An} = L_{Cat} = 1.138$ cm. The center compartment in the 3C reactor included the thickness of the surrounding gaskets (L_C = 0.856 cm). R_{meas} is the sum of the individual resistances, or

$$R_{meas} = R_{soln,An} + n\ R_{mem} + R_{soln,C} + R_{soln,Cat} \tag{3.5}$$

where n is the number of membranes (n = 1 for the 2C system, and n = 2 for the 3C system). R_{mem} is the membrane resistance, which is obtained as:

$$R_{mem} = \frac{R_{meas} - R_{soln,An} - R_{soln,C} - R_{soln,Cat}}{n} \tag{3.6}$$

Membrane area-resistance was calculated as $R_{mem,A} = R_{mem}\, A_G$, where A_G = 6.55 cm^2 is the measured area of the gasket.

The resistance of the center compartment (R_c) can be used to determine the resin conductivity (σ_{resin}). When $\emptyset_{resin} \neq 0$, the center compartment resistance is calculated from measured resistance as $R_{meas} = R_{soln,An} + 2\, R_{mem} + R_C + R_{soln,Cat}$. The resin ($R_{resin}$) and solution resistance in the center chamber act like resistors in a parallel circuit, and therefore:

$$\frac{1}{R_C} = \frac{1}{R_{soln,C}} + \frac{1}{R_{resin}} \tag{3.7}$$

The resistance of the resin in the center chamber (R_{resin}) can be expressed as a function of the resin conductivity as:

$$R_{resin} = \frac{L_C}{A\, \sigma_{resin} \emptyset_{resin}} \tag{3.8}$$

Rearranging, and using equations 3.7, and 3.2, the conductivity of the resin can be calculated as:

$$\sigma_{resin} = \frac{L_C}{A\, R_C\, \emptyset_{resin}} - \sigma_{soln,C}\left(\frac{1}{\emptyset_{resin}} - 1\right) \tag{3.9}$$

The average resin conductivity ($\overline{\sigma}_{resin}$) was calculated from individual measurements using different volumes of resin ($\emptyset_{resin}$). The resistance of the center chamber, on average ($R_{C,fit}$), can therefore be predicted using $\overline{\sigma}_{resin}$ and equations 3.5, 3.7, and 3.8, as:

$$\frac{1}{R_{C,fit}} = \frac{A\, \emptyset_{resin}\, \overline{\sigma}_{resin}}{L_C} + \frac{A\, (1 - \emptyset_{resin})\, \sigma_{soln,C}}{L_C} \tag{3.10}$$

After rearrangement, the predicted average resistance as a function of the resin volume is:

$$R_{C,fit} = \frac{L_C}{A\, \emptyset_{resin}\, \overline{\sigma}_{resin} + (1 - \emptyset_{resin})\, \sigma_{soln,C}} \tag{3.11}$$

In the mixed-resin system, the $R_{C,fit}$ was estimated based on the average resin conductivity ($\overline{\sigma}_{resin,avg}$) of the AH and CH systems, calculated as:

$$\overline{\sigma}_{resin,avg} = \frac{\overline{\sigma}_{resin,AH} + \overline{\sigma}_{resin,CH}}{2} \tag{3.12}$$

where $\overline{\sigma}_{resin,AH}$ and $\overline{\sigma}_{resin,CH}$ were the AH and CH average resin conductivities.

Chapter 4

Results

4.1 Ion Exchange Membrane Resistance in NaCl Systems

The 3C reactor was tested with HC and LC NaCl solutions and Selemion AMVs and CMVs to determine if the calculated membrane resistances were similar to previous results [55, 56], and therefore if the system was functioning as expected. The Selemion AMV had a resistance of 64 ± 13 Ω-cm^2, which favorably compared to that of Geise et al. [56] who calculated a resistance of 49 ± 20 Ω-cm^2 for the same membrane and NaCl conditions. The Selemion CMV had a resistance of 52 ± 15 Ω-cm^2. This was lower than the 76 ± 21 Ω-cm^2 obtained by Geise et al. [56] under the same conditions, and higher than the 42 Ω-cm^2 reported by Galama et al. [55] using 0.9 M (HC) and 10 mM (LC) NaCl solutions on either side of one membrane, compared to 1 M and 10 mM used here. These results indicated that the membrane resistances could be accurately measured, although there were relatively large standard errors associated with measurements.

4.2 Ion Exchange Resin Conductivity

Using the 3C reactor, ion exchange resin conductivity (equation 3.9) was calculated for AH, AL, CH, and CL resins. The AH resin produced the highest conductivity of all resins tested, of 11.7 ± 2.9 mS/cm. AL resin had an average conductivity of 8.8 ± 0.5 mS/cm, and the CL resin had an average conductivity of 9.2 ± 0.5 mS/cm. The CH resin had the lowest average conductivity of 7.0 ± 1.0 mS/cm, which was opposite what was expected as this resin had a high IEC [53].

There was an 81.7% reduction in R_C, from 97.2 ± 0.0 to 17.6 ± 0.1 Ω, when the AH resin was used with $\emptyset_{resin}$= 0.5 (Figure 4.1). There was relatively good agreement between the resistances measured for this resin at different volume fraction with that predicted based on an average resin conductivity ($\overline{\sigma}_{resin}$ = 11.7 mS/cm) using equation 3.11 (Figure 4.1). Using this equation, it can be seen that there would be little further reduction in the center chamber resistance after using more than ~50% of the chamber was filled with resin.

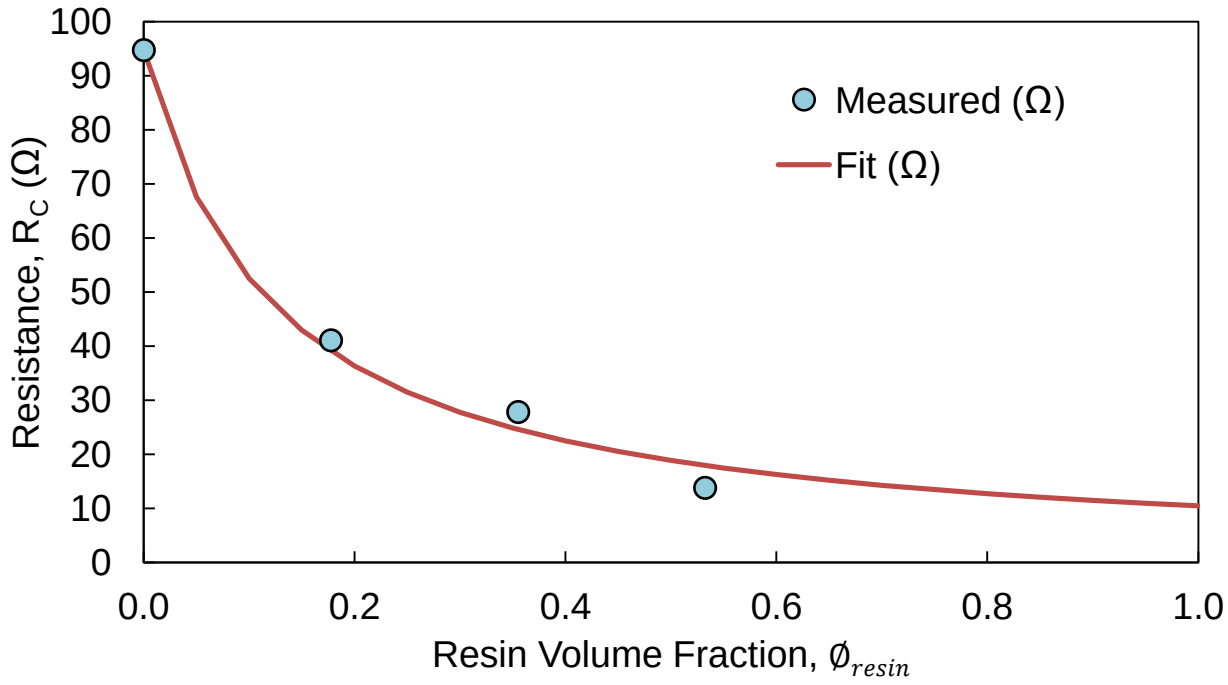

Figure 4.1. The center compartment resistance (R_C) is based on the resin volume fraction ($\emptyset_{resin}$). Increasing high IEC anion exchange resin (1X8) volume in the center chamber of a sodium chloride (NaCl) system improved performance by decreasing resistance. The fit ($R_{C,fit}$) is based on an average resin conductivity of 11.7 mS/cm.

A 3C reactor, filled 50% by volume with equal masses of AH and CH resins, was also tested to see if a mixed resin could further reduce resistance. The resin conductivity was expected to be an average of the AH and CH conductivities, or $\overline{\sigma}_{resin,avg}$ = 9.4 mS/cm. However, there was poor agreement between the expected resistance ($R_{C,fit}$) with data obtained

using the mixed resin (Figure 4.2). A best fit of the mixed resin results indicated that the mixed resin had on average a conductivity of $\overline{\sigma}_{resin} = 3.1 \pm 1.0$ mS/cm. This lower conductivity suggested that the presence of both the anionic and cationic resin impeded charge transfer through the middle chamber.

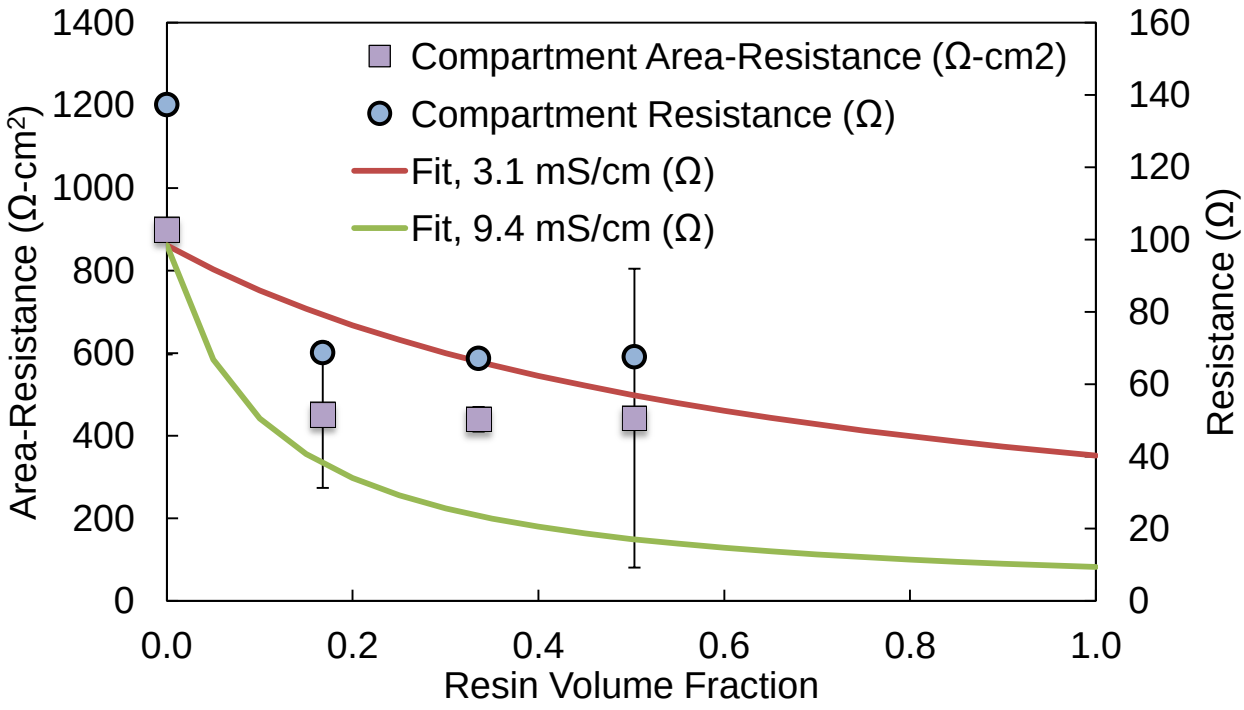

Figure 4.2. A sodium chloride (NaCl) system with mixed high IEC resin (50% anion, 50% cation) had an expected resistance ($R_{C,fit}$ using an average for the two resins of $\overline{\sigma}_{resin,avg}$ = 9.4 mS/cm). However, the data show best agreement with a lower conductivity using $R_{C,fit}$ and $\overline{\sigma}_{resin}$ = 3.1 mS/cm).

4.3 Center Chamber Flow Rate

The effect of the center chamber flow rate on membrane resistance was measured in the 3C reactor using two AEMs with and without AH resin in the center chamber. Without resin in the center chamber, AEM resistance increased by 14% to 85 ± 8.7 Ω-cm^2 when flow rate increased from 2 mL/min to 8 mL/min (Figure 4.3a). These flow rates equate to HRTs of 3.1 min

to 47 s (Figure 4.3b). Under the same HRTs with AH resin for $\emptyset_{resin}$= 0.5, or flow rates 1-4 mL/min, AEM resistance increased by 10% to 78 ± 3.8 Ω-cm^2. At the highest flow rate (30 mL/min) without resin, membrane resistance increased to 110 Ω-cm^2. When the center chamber was filled with resin, flow rates above 7 mL/min caused resin to flow out of the center chamber so the resistances could not be accurately measured.

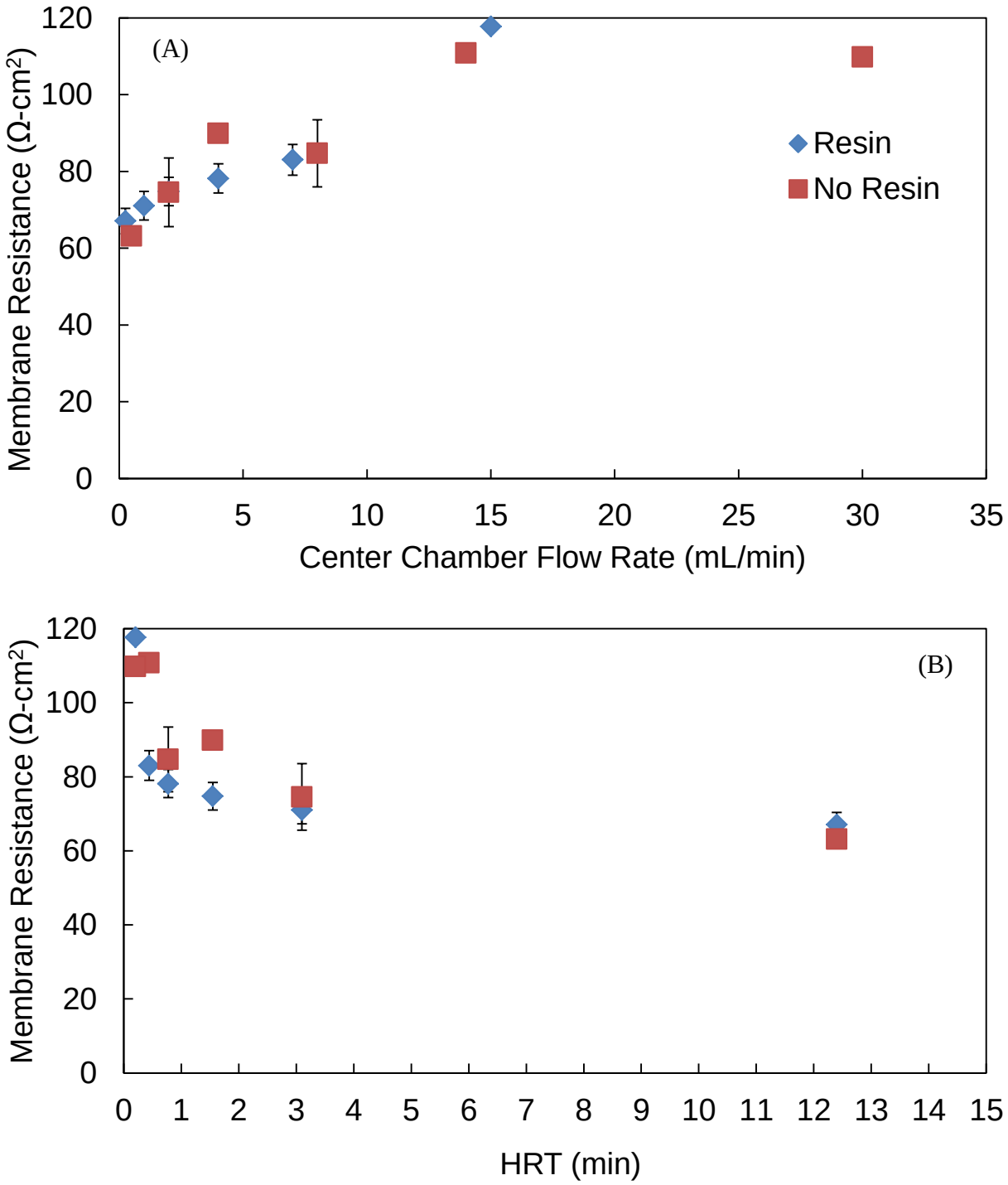

Figure 4.3: (A) Membrane resistance as a function of flowrate and (B) HRT in the LC chamber.

Another test was performed with center chamber flow rates of 2-8 mL/min, and solution conductivity was measured at the outlet to calculate changes in membrane resistance. The solution conductivity increased between 1-3% at the outlet with and without resin. Although the

conductivity change was small, calculated membrane resistance increased by up to 23% if the outlet conductivity was used in calculations. When using the average conductivity of inlet and outlet solution, the calculated membrane resistance increased at most by 12% (Figure 4.4).

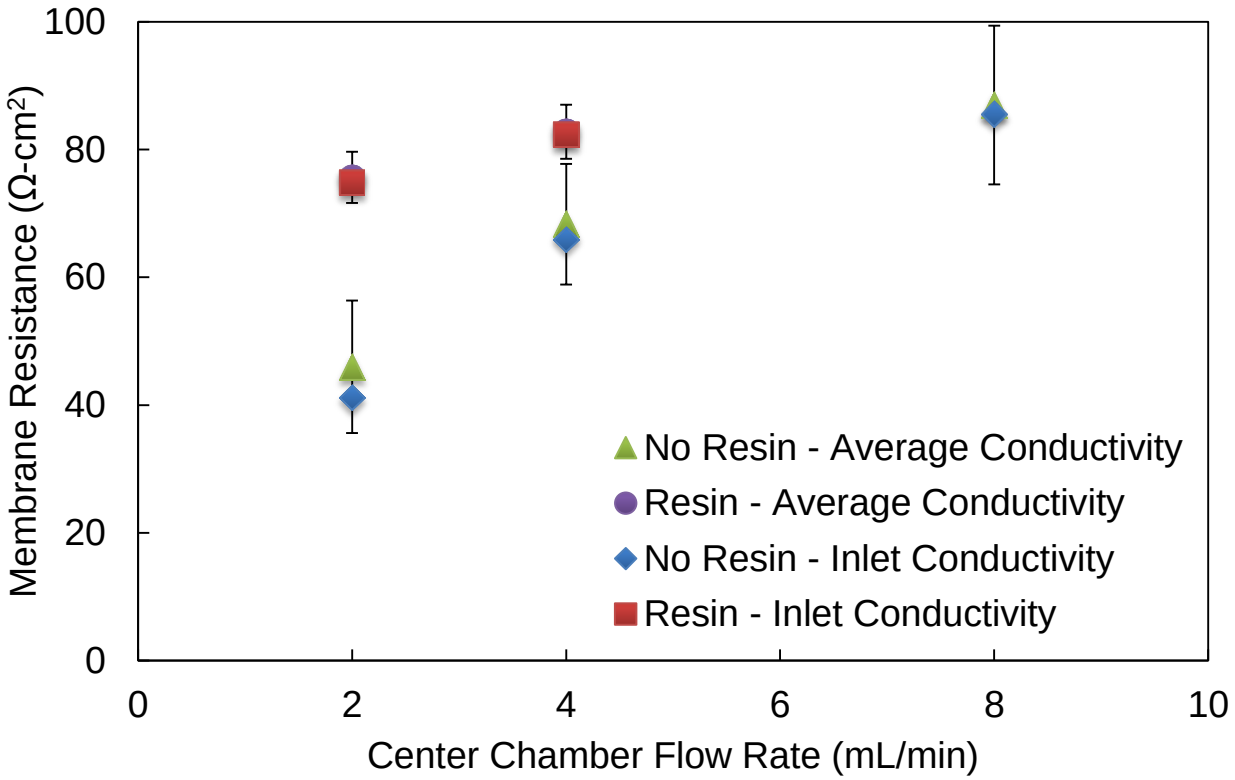

Figure 4.4. Calculated membrane resistance increases when using the average of the low concentration solution inlet and outlet conductivities.

4.4 Nitrogen Crossover

Nitrogen crossover was measured in the 3C reactor using 50% of the center chamber filled by the AH resin (HC | LC + R | B) and two AEMs. The TAN concentration was reduced by 96.5% to 26 ± 7 mg/L after 24 h when using resin and these membranes, compared to the control (HC | B) lacking the center chamber (741 ± 39 mg/L) (Figure 4.4). This reduced crossover was also 36% less than that obtained using a center chamber with no resin (HC | LC | B), though the majority of the crossover mitigation was a result of the LC chamber instead of resin. In an

MREC using AmB, carbamate ions cross from the high concentration chamber into the anode chamber due to the concentration and electric gradients [10]. The 2C reactor replicated these conditions of an anode adjacent to a high concentration RED cell of an MREC (HC | B) separated by an AEM. These results show that nitrogen crossover can be greatly reduced by using an additional LC chamber (two AEMs) with an anion exchange resin with a high ion exchange capacity.

Anode pH in the 3C reactor with resin increased from 8.5 to 10.4 ± 0.0, which was different from that which would occur in a typical MREC where pH decreases (Figure 4.4) [10, 45]. In the 3C reactor without resin, the anode pH increased to 10.5 ± 0.1, which was similar to the system with resin. In the control 2C reactor, the anode pH decreased from 10.7 to 9.9 ± 0.3. This pH decrease resulted from water electrolysis at the platinum electrode.

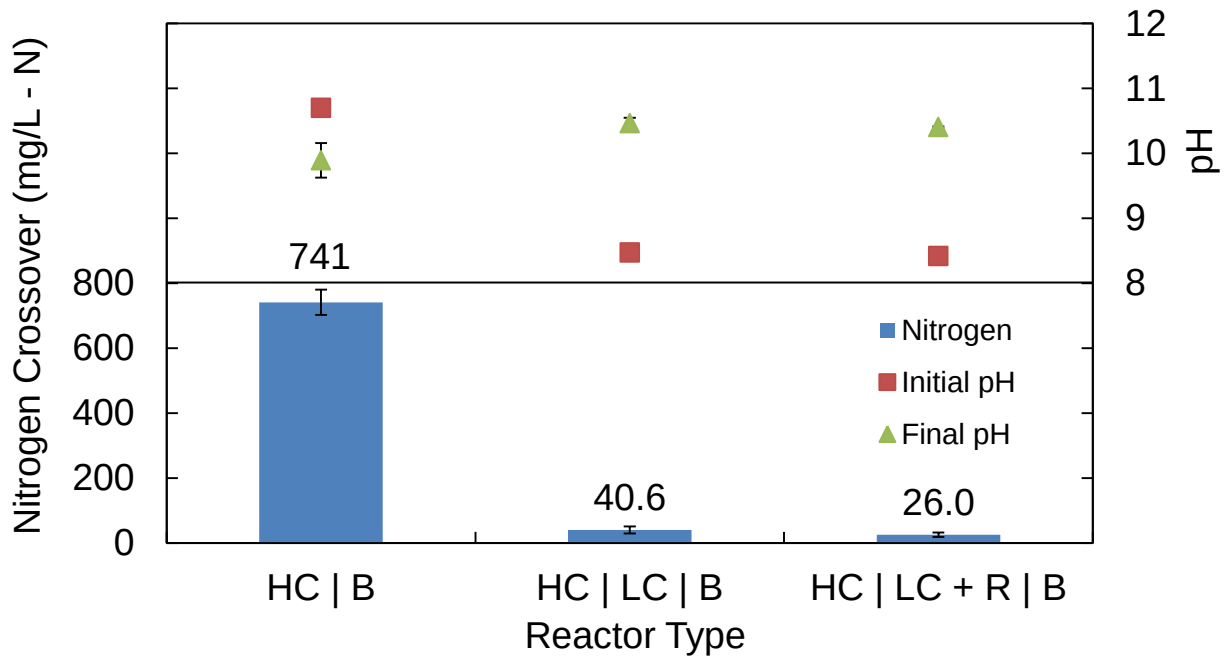

Figure 4.5. Nitrogen crossover into anode chamber was severely reduced when adding the low concentration chamber next to the anode. Anode chamber pH increased in this system, which may adversely affect microbial growth.

4.5 Low concentration chamber resistance with ammonium bicarbonate

While the use of a low concentration chamber can reduce nitrogen crossover, it increases the overall system internal resistance. The resistance due to membranes was 2.9× higher in the 3C reactor (295 ± 37 Ω-cm^2) than the 2C reactor (103 ± 18 Ω-cm^2) (Figure 4.5). The Selemion AMV resistance in the 2C reactor was lower than the ~115 ± 20 Ω-cm^2 reported by Geise et al. [59] using less conductive solutions, which was expected because membrane resistance decreases when using a higher conductivity solution.

When 50% of the LC chamber volume was filled with AH resin (HC | LC + R | B), the LC chamber resistance was 166 ± 9 Ω-cm^2, which was a 74% decrease compared to the reactor containing solution without resin (Figure 4.5). The majority of the resistance (64%) came from the membranes, with a total resistance of 461 ± 38 Ω-cm^2 for membranes and solution. Without the resin in the LC chamber (HC | LC | B), the solution resistance was much higher (637 ± 35 Ω-cm^2). The membrane resistance was the same, so the majority of the resistance in the absence of the resin (68%) was due to the low conductivity solution. The resistance of the 2C reactor (HC | B) was lower than either of the 3C configurations (with or without resin) because there was no resistance due to a LC solution or additional membrane.

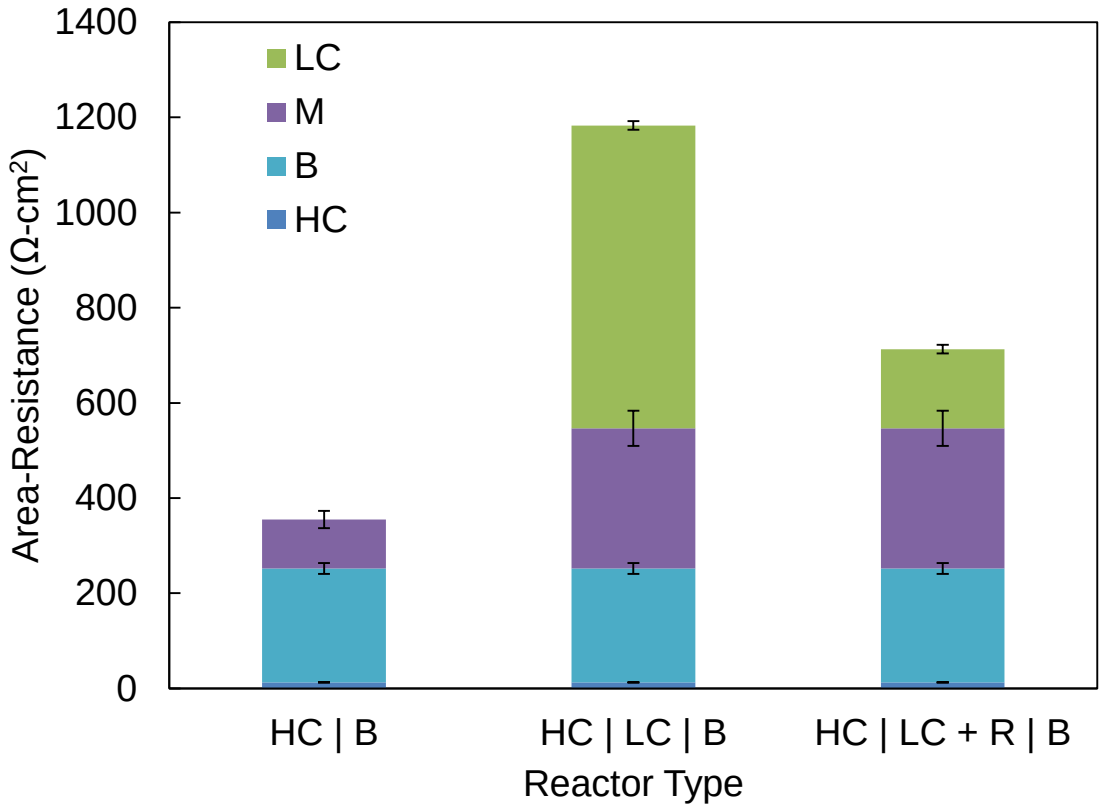

Figure 4.6. The area-resistance of the 2C and 3C reactors using ammonium bicarbonate. The third reactor contained resin (R). The reactors are comprised of the low concentration (LC) chamber, membranes (M), buffer (B), and high concentration (HC) solution.

Chapter 5

Discussion

5.1 Impacts of Membranes on Resistance

The AEM resistance between AmB and buffer solutions was greater than when it was placed in between HC and LC NaCl solutions. Typically, membrane resistance is lowest when it is placed in between high conductivity solutions. If a solution on one side of the membrane has a lower conductivity, the membrane resistance increases [55, 56]. When comparing membrane resistances using the LC NaCl or the buffer solution conductivities, the AEM resistance when it was placed between buffer ($\bar{\sigma} = 4.3$ mS/cm) and HC ($\bar{\sigma} = 80.0$ mS/cm) AmB (103 ± 18 Ω-cm^2) was higher than when in between HC ($\bar{\sigma} =$ 86.8 mS/cm at 25 °C) and LC ($\bar{\sigma} =$ 1.07 mS/cm at 25 °C) NaCl (64 ± 13 Ω-cm^2) despite the higher conductivity of the buffer. This increased AEM resistance when exposed to AmB was likely due to the decreased mobility of the anions in AmB [56, 59]. In the 3C reactor with HC and LC AmB and buffer, membrane resistance increased to 295 ± 37 Ω-cm^2 due to the additional membrane placed between two very low conductivity solutions, buffer ($\bar{\sigma} = 4.3$ mS/cm) and LC AmB ($\bar{\sigma} = 1.2$ mS/cm). Membrane conductivity decreases significantly when it is used in low conductivity solutions [55, 56] . The high resistance that results from using AEMs exposed to low conductivity solutions would decrease energy efficiency of an MREC.

5.2 Impacts of Ion Exchange Resin on Resistance

The anionic, high IEC resin (AH) reduced the LC chamber resistance in 3C reactors using either NaCl or AmB in the LC chamber. When AH resin was used in the NaCl LC chamber, the chamber resistance was reduced by 81.7% to 115 ± 1 Ω-cm^2. In the reactor using

AmB in the LC chamber, resistance was reduced by 74% to 166 ± 9 Ω-cm^2 with the same resin type. The use of the AH resin decreased the resistance of the additional LC chamber by approximately the same amount in both solution cases (NaCl and AmB). Thus, the effects of ion exchange resin on the AmB LC chamber could be closely approximated using the results of only the NaCl LC chamber. Even with the reduction in LC chamber resistance, the total resistance was still higher than a system without the additional chamber; however, the LC chamber was necessary in order to reduce nitrogen crossover.

The LC chamber resistance could be further reduced because the cell thickness in this study (8.56 mm) was very large compared to a standard RED stack [28, 60]. The cells in previous lab-scale MRECs were 85% thinner (1.3 mm) [13]. The chamber width (L_C) could be reduced to the gasket width in this study (1.58 mm) so a new theoretical area-resistance for the chamber can be estimated using equation 3.8. For the LC chamber of the AmB reactor the reduced area-resistance would be 30 Ω-cm^2 compared to 166 Ω-cm^2, which would help increase energy efficiency. However, reducing the width of the chamber would likely increase nitrogen crossover.

A further reduction in an LC chamber resistance could likely be obtained by using resins with a higher IEC. Three factors determine ion exchange resin conductivity: a high concentration of fixed ionic groups, a low degree of cross-linkage, and the use of small size and low valence counter ions in the resin [53]. The AH resin was 33% more conductive than the AL resin. This was due to the high concentration of fixed groups (1.2 meq/L), or IEC, and despite the higher degree of cross-linkage (Table 3.2). A resin with higher IEC may be more conductive the AH resin. For example, two potential anionic Dowex resins with higher IECs are Marathon A (1.3 meq/L) and Marathon 11 (1.3 meq/L) [61].

The beneficial effect of adding resin to reduce the LC chamber resistance was relatively small when more than 50% of the chamber was filled with resin (Figure 4.1). The compartment resistance approached a minimum limit when increasing the volume of resin, as shown by equation 3.6. To optimize the use of resin, relative to benefits versus the cost of the resin, no more than 50% of the chamber needs to be filled.

5.3 Impacts of Flow Rate on Membrane Resistance

Increasing the LC center chamber flowrate in the 3C reactor increased membrane resistance. The decreased resistance at low flow rates was due to salt crossover, which affected the solution concentration differences enough to decrease membrane resistance [56]. At high HRTs (47 s – 12.4 m) there was very little difference in membrane resistance between the 3C reactor with and without resin, even considering what appeared to be an outlier at 1.55 min (Figure 4.3b). At an HRT of 27 s, the system with resin had lower membrane resistance than the system without, likely due to the resin impacting the boundary layer conditions of the higher flow rate. However at the lowest HRT (12 s), resin fluidized and flowed out of the center chamber, so membrane resistance recorded at this point was not accurate. In one test, the presence of resin had little effect on calculated membrane resistance for similar flow rates (Figure 4.3a). However in a second test, membrane resistance increased by almost 82% when resin was added at low flow rates (Figure 4.4). Additionally, the resistance increased up to 11% when accounting for solution conductivity changes. The discrepancies between membrane resistance measured under the same flow rates and solution conditions show the difficulties in measuring ion exchange membrane resistance at low flow rates and with low conductivity solutions. This means that there is a larger uncertainty in membrane and ion exchange measurements, which were taken at lower flow rates. However, resistance in nitrogen tests was

largely unaffected because at the HRT (1.55 min) and flow rates (2-4 mL/min) tested, there was little change in measured membrane resistance (Figure 4.3, Figure 4.4). Overall, the membrane resistance changes were too small to change the overall conclusions regarding membrane resistance and ion exchange resin conductivity.

5.3 Nitrogen Crossover and pH Changes

The addition of an LC chamber using an AEM and filled 50% with AH resin was successful in reducing nitrogen crossover in the 3C AmB reactor. The TAN concentration after 24 h was reduced by 96.5%, from 741 mg/L to 26 mg/L, due to the LC chamber and resin (Table 5.1). In previous MRECs, the HC chamber adjacent to the anode created a concentration gradient that drove negative ions like carbamate into the anode [10, 13]. With the LC solution adjacent to the anolyte, it is thought that charge was also balanced by the transport of negative ions through the AEM and out of the anode chamber. This would have reduced negative ion transfer from the LC chamber into the anolyte, and thus the transfer of carbamate into the anolyte. Luo et al. [13] reduced nitrogen crossover by 60%, to a final concentration of 311 mg/L, by using an additional LC chamber with a CEM adjacent to the anode chamber. The different results obtained here are due to the use of the AEM, compared to the CEM, adjacent to the anolyte. The system by Luo et al. [13] likely resulted in more nitrogen transfer into the anolyte due to NH_4^+ ion transfer. In the LC cell, at the pH (7) and temperature (28 °C) of the AmB solution used, NH_4^+ has a significantly higher (> 5×) concentration than carbamate [62]. Thus, the use of a CEM adjacent to the anode in the configuration used by Luo et al. [13] would result in transfer of NH_4^+ into the anode chamber due to its ability to pass through the adjacent CEM.

The additional LC chamber without resin was also successful in reducing nitrogen crossover simply because the concentration gradient between the buffer and LC solution

minimized carbamate transfer into the anolyte. Nitrogen crossover was reduced by 94.5% using the additional LC chamber with an AEM. This showed the majority of the crossover mitigation resulted from the AEM being placed in between the LC chamber and anode.

Table 5.1: Comparison of TAN crossover and coulombs transferred after one cycle in MRECs and this study

System	AmB Concentration (M)	Coulombs Transferred	Anode TAN (mg/L)	Reference
MREC	1.8	346	590	Cusick et al. [10]
MREC	1.7	192	789	Luo et al. [13]
MREC + LC (0.023 M)	1.7 With 0.023 LC Chamber	242	311	
MREC	1.1	346	741	This study
MREC + LC (0.011 M)	1.1 With 0.011 LC Chamber	346	40.6	
MREC + LC (0.011 M) + Resin	1.1 With 0.011 LC Chamber and 50% Dowex 1X8	346	26.0	

The anode chamber pH increased when using the 3C reactor due to the additional LC chamber. In both cases of the 3C reactor (with and without resin), anolyte pH increased from 8.5 to around 10.5 after 24 h. There are two potential causes of this pH shift: protons leaving the anode chamber, and protons combining with negatively charged bicarbonate species. Protons may have exited the anode chamber through the AEM to balance the charge lost from negative ionic species transferring out of the anode chamber. This is possible because the Selemion AMV is not 100% permselective. It is also possible that protons combined with HCO_3^-, a species present in AmB [49], that could have transferred into the anode chamber from the LC AmB solution. Jadhav et al. [63] observed that for anodes in a neutral pH (6.5) the anolyte generated a greater current than higher (7.0, 7.5) or lower (6.0, 5.5) pH anolytes. As most MFCs operate with

a neutral anolyte pH, the severe pH rise observed in the 3C reactor will likely decrease performance.

5.4 Estimated Power Losses and Mitigation

The increased resistance due to the additional LC chamber and AEM will decrease the energy efficiency of an MREC. The extent of power loss can be estimated based on the increased resistance using an additional chamber and membrane. Based on net power equations for RED stacks [28], the power loss (P_{loss}) is:

$$P_{loss} = \frac{(R_{soln} + R_{mem})}{A_G} \cdot j^2 \tag{5.1}$$

where here j = 4 mA, R_{soln} = 30 Ω-cm^2 due to the modified width (1.58 mm) LC chamber (section 5.2), R_{mem} = 192 Ω-cm^2 due to the additional AEM, and A_G = 6.55 cm^2. The resistance due to the additional AEM was the difference between the membranes in the 3C reactor (295 Ω-cm^2) and 2C reactor (103 Ω-cm^2). This modified area-resistance took into consideration ohmic (R_{ohmic}), bulk concentration change ($R_{\Delta C}$), and boundary layer (R_{BL}) resistances for membranes. Power loss was 0.544 mW for the additional AEM and LC NaCl solution.

Power loss can be mitigated by introducing additional membranes to the RED stack. The number of membranes necessary to mitigate power loss from the solution and membrane resistances [28] is:

$$P_{net} = N_{pairs}\, E_{OCV}\, j - P_{loss} - \frac{N_{pairs}\,(R_{soln} + R_{mem}) j^2}{A_G} \tag{5.2}$$

where P_{net} is the net power (set at zero), and N_{pairs} the number of membrane pairs. Based on a current of j = 4 mA, P_{loss} = 0.544 mW, E_{OCV} = 0.156 V [25, 26] for one membrane pair (one AEM and one CEM), R_{mem} = 140 Ω-cm^2 for the membrane pair [56], R_{soln} = 30 Ω-cm^2

considering HC solution is negligible, and A_G = 6.55 cm^2, three additional membrane pairs (N_m= 2.75, rounded to nearest integer) in an MREC could be used mitigate the power loss due to the use of the additional LC cell. The addition of six membranes to overcome power loss due to resistance is therefore substantial if the stack size is only a few membranes [10], but relatively insignificant if a large RED stack of several hundred membrane pairs are used.

Power losses can also arise in a stack due to the formation of bubbles when AmB is used [43]. When bubbles form, the gas prevents liquid contact with the membrane, and thus the ion exchange capacity of the membranes is reduced. Altering the chamber design can minimize bubble formation [43]. However, the ion exchange resin could introduce a greater number of pores for bubbles to form in and become lodged in the resin. This inclusion of bubbles in the resin chamber could increase internal resistance, and decrease the overall energy efficiency of the system.

Power is also lost to pumping energy required in the stack, and that needed to pump solutions to and from the stack. Pumping losses within the stack have previously been studied in RED, and they were estimated to increase the power loss by 25% in larger systems [29, 44]. When resin is added to the LC chamber, additional pumping losses are introduced. The pressure drop due to the flow in a packed bed of resin can be estimated using the Kozeny-Carman equation and available data for pressure drop based on resin size. Large resin particles (smaller mesh) will have a smaller pressure drop (Figure 5.1), so larger resins are desirable from the perspective of energy losses due to pumping.

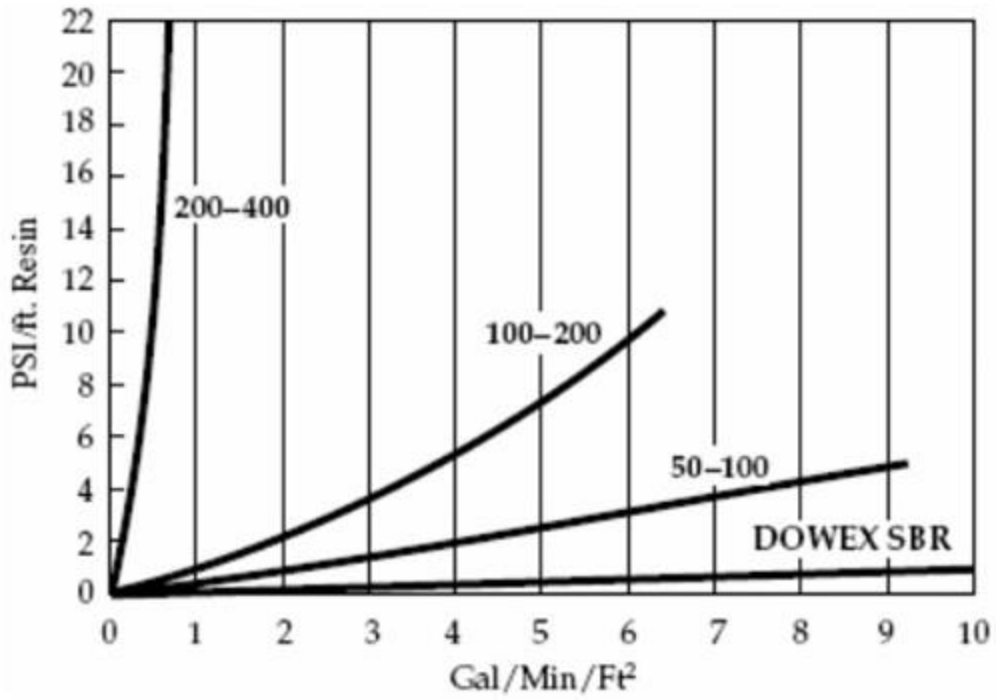

Figure 5.1. The ion exchange resin mesh significantly changes the pressure drop, and therefore power loss, in the system. Smaller mesh (larger) resins have smaller pressure drops. Taken from Dow Water Solutions [64].

Chapter 6

Conclusions

Installing an additional AEM to create an LC (11 mM AmB) chamber between the anode chamber and HC (1.1 M) AmB successfully reduced nitrogen crossover by minimizing carbamate transfer into the anolyte. With the addition of 50% by volume Dowex 1X8 ion exchange resin to the LC chamber, nitrogen crossover was reduced by 96.5% (from 741 mg/L) to 26 mg/L TAN. Nitrogen crossover was reduced by 94.5% when using the LC chamber without resin. The addition of an LC cell reduced nitrogen crossover greater than that previously achieved [13] because the concentration gradient between the LC chamber and anode reduced negatively charged carbamate transfer into the anode.

The use of ion exchange resin reduced some of the resistance introduced by the additional LC chamber. Dowex 1X8, which is anionic and has a high IEC, reduced solution resistance by 74% (from 637 Ω-cm^2 to 166 Ω-cm^2). Resistance due to AEMs increased by 186% to 295 Ω-cm^2 because the additional membrane was between low conductivity solutions (buffer and the LC solutions). The use of the ion exchange resin was successful in reducing solution resistance, but AEM resistance increased greatly because of the low conductivity solutions.

Chapter 7

Future Work

The internal resistance can be further reduced by increasing the conductivity of the system, which would increase the total net power. Conductivity could be improved by:

- Increasing AEM conductivity in AmB and LC solutions by tailoring permselectivity and resistance.
- Using an alternative commercial membrane to Selemion that has lower resistance and better permselectivity for AmB.
- Using an alternative, electrically conductive material instead of ion exchange resin because its desalination properties are not required.

Nitrogen crossover was reduced here, but it would need to be further reduced if wastewater was used in the anode chamber in order to meet effluent nitrogen standards (<5-10 mg/L). One option for further nitrogen crossover mitigation includes adding a second LC chamber to further reduce the concentration of nitrogen that is potentially present next to the anode chamber, although this would require adding additional membrane pairs into the stack to offset the reduction in power that would occur with this addition LC chamber.

BIBLIOGRAPHY

[1] World population prospects: The 2012 revision, highlights and advance tables, United Nations, Department of Economic and Social Affairs, Population Division, 2013.
[2] International energy statistics, U.S. Energy Information Administration, www.eia.gov, 2012.
[3] Estimated U.S. energy use in 2013: ~97.4 quads, Lawrence Livermore National Laboratory and Department of Energy, www.llnl.gov, 2014.
[4] How much carbon dioxide is produced when different fuels are burned?, EIA, www.eia.gov, 2014.
[5] R.K. Pachauri, et al., Climate change 2014 synthesis report, in: R.K. Pachauri, L. Meyer (Eds.) Fifth Assessment Report (AR5), Intergovernmental Panel on Climate Change, www.ipcc.ch, 2014.
[6] Water & sustainability: U.S. electricity consumption for water supply & treatment - The next half century, EPRI, Palo Alto, CA, 2000.
[7] Emefcy, EBR - Electrogenic bio reactor, Emefcy, emefcy.com.
[8] B.E. Logan, Microbial fuel cells, John Wiley & Sons, Inc., Hoboken, NJ, 2008.
[9] A.J. Hutchinson, J.C. Tokash, B.E. Logan, Analysis of carbon fiber brush loading in anodes on startup and performance of microbial fuel cells, *J. Power Sources*, 196 (2011) 9213– 9219.
[10] R.D. Cusick, Y. Kim, B.E. Logan, Energy capture from thermolytic solutions in microbial reverse-electrodialysis cells, *Science*, 335 (2012) 1474-1477.
[11] R.L. McGinnis, J.R. McCutcheon, M. Elimelech, A novel ammonia-carbon dioxide osmotic heat engine for power generation, *J. Mem. Sci.*, 305 (2007) 13-19.
[12] J.-Y. Nam, H.-W. Kim, H.-S. Shin, Ammonia inhibition of electricity generation in single-chambered microbial fuel cells, *J. Power Sources*, 195 (2010) 6428-6433.
[13] X. Luo, et al., Optimization of membrane stack configuration for efficient hydrogen production in microbial reverse-electrodialysis electrolysis cells coupled with thermolytic solutions, *Bioresour. Technol.*, 140 (2013) 399-405.
[14] A. Morel, et al., Microbial desalination cells packed with ion-exchange resin to enhance water desalination rate, *Bioresour. Technol.*, 118 (2012) 43-48.
[15] K. Zuo, L. Yuan, J. Wei, P. Liang, X. Huang, Competitive migration behaviors of multiple ions and their impacts on ion-exchange resin packed microbial desalination cell, *Bioresour. Technol.*, 146 (2013) 637-642.
[16] K. Zuo, et al., A ten liter stacked microbial desalination cell packed with mixed ion-exchange resisn for secondary effluent desalination, *Environ. Sci. Technol.*, 48 (2014) 9917-9924.
[17] N. Shehab, G. Amy, B.E. Logan, P.E. Saikaly, Enhanced water desalination efficiency in an air-cathode stacked microbial electrodeionization cell (SMEDIC), *J. Mem. Sci.*, 469 (2014) 364-370.
[18] F. Zhang, M. Chen, Y. Zhang, R.J. Zeng, Microbial desalination cells with ion exchange resin packed to enhance desalination at low salt concentration, *J. Mem. Sci.*, 417–418 (2012) 28-33.
[19] K. Rabaey, W. Verstraete, Microbial fuel cells: Novel biotechnology for energy generation, *Trends Biotechnol.*, 23 (2005) 291-298.
[20] B.E. Logan, et al., Microbial fuel cells: Methodology and technology, *Environ. Sci. Technol.*, 40 (2006) 5181-5192.

[21] MFC schematic, The Biodesign Institute at Arizona State University, asunews.asu.edu, 2012.
[22] R.E. Pattle, Production of electric power by mixing fresh and salt water in the hydroelectric pile, *Nature*, 174 (1954) 660.
[23] D.A. Vermaas, D. Kunteng, M. Saakes, K. Nijmeijer, Fouling in reverse electrodialysis under natural conditions, *Water Res.*, 47 (2013) 1289-1298.
[24] B.E. Logan, M. Elimelech, Membrane-based processes for sustainable power generation using water and wastewater *Nature*, 288 (2012) 313-319.
[25] J. Veerman, J. Post, M. Saakes, S. Metz, G. Harmsen, Reducing power losses caused by ionic shortcut currents in reverse electrodialysis stacks by a validated model., *J. Mem. Sci.*, 310 (2008) 418-430.
[26] J. Veerman, R.M. de Jong, M. Saakes, S.J. Metz, G.J. Harmsen, Reverse electrodialysis: Comparison of six commercial membrane pairs on the thermodynamic efficiency and power density, *J. Mem. Sci.*, 343 (2009) 7-15.
[27] ClimateTechWiki, Schematic representation of the RED process, climatetechwiki.org.
[28] D.A. Vermaas, E. Guler, M. Saakes, K. Nijmeijer, Theoretical power density from salinity gradients using reverse electrodialysis, *Energy Procedia*, 20 (2012) 170-184.
[29] J. Veerman, M. Saakes, S.J. Metz, G. Harmsen, Revese electrodialysis: Performance of a stack with 50 cells on the mixing of sea and river water, *J. Mem. Sci.*, 327 (2008) 136-144.
[30] J.N. Weinstein, F.B. Leitz, Electric power from differences in salinity: The dialytic battery, *Science*, 191 (1976) 557-559.
[31] R.E. Lacey, Energy by reverse electrodialysis, *Ocean Eng.*, 7 (1980) 1-47.
[32] P. Długołecki, J. Dabrowska, K. Nijmeijer, M. Wessling, Ion conductive spacers for increased power generation in reverse electrodialysis, *J. Mem. Sci.*, 347 (2010) 101-107.
[33] D.A. Vermaas, M. Saakes, K. Nijmeijer, Enhanced mixing in the diffusive boundary layer for energy generation in reverse electrodialysis, *J. Mem. Sci.*, 453 (2014) 312-319.
[34] P. Długołęcki, K. Nymeijer, Current status of ion exchange membranes for power generation from salinity gradients, *J. Mem. Sci.*, 319 (2008) 214-222.
[35] G.M. Geise, H.J. Cassady, D.R. Paul, B.E. Logan, M.A. Hickner, Specific ion effects on membrane potential and the permselectivity of ion exchange membranes, *Phys. Chem. Chem. Phys.*, 16 (2014) 21673-21681.
[36] N.Y. Yip, M. Elimelech, Comparison of energy efficiency and power density in pressure retarded osmosis and reverse electrodialysis, *Environ. Sci. Technol.*, 48 (2014) 11002-11012.
[37] G.M. Geise, M.A. Hickner, B.E. Logan, Ionic resistance and permselectivity tradeoffs in anion exchange membranes, *ACS Appl. Mat. Interfac.*, 5 (2013) 10294-10301.
[38] E. Güler, Y. Zhang, M. Saakes, K. Nijmeijer, Tailor-made anion-exchange membranes for salinity gradient power generation using reverse electrodialysis, *ChemSusChem*, 5 (2012) 2262-2270.
[39] E. Güler, R. Elizen, D.A. Vermaas, M. Saakes, K. Nijmeijer, Performance-determining membrane properties in reverse electrodialysis, *J. Mem. Sci.*, 446 (2013) 226-276.
[40] D.A. Vermaas, M. Saakes, K. Nijmeijer, Power generation using profiled membranes in reverse electrodialysis, *J. Mem. Sci.*, 385-386 (2011) 234-242.
[41] J. Liu, et al., Patterned ion exchange membranes for improved power production in microbial reverse-electrodialysis cells, *J. Power Sources*, 271 (2014) 437-443.
[42] X. Luo, et al., Power generation by coupling reverse electrodialysis and ammonium bicarbonate: Implication for recovery of waste heat, *Electrochem. Commun.*, 19 (2012) 25-28.

[43] M.C. Hatzell, B.E. Logan, Evaluation of flow fields on bubble removal and system performance in an ammonium bicarbonate reverse electrodialysis stack, *J. Mem. Sci.*, 446 (2013) 449-455.
[44] Y. Kim, B.E. Logan, Microbial reverse electrodialysis cells for synergistically enhanced power production, *Environ. Sci. Technol.*, 45 (2011) 5834-5839.
[45] Y. Kim, B.E. Logan, Hydrogen production from inexhaustible supplies of fresh and salt water using microbial reverse-electrodialysis electrolysis cells, *Proc. Natl. Acad. Sci. USA*, 108 (2011) 16176-16181.
[46] J.-Y. Nam, R.D. Cusick, Y. Kim, B.E. Logan, Hydrogen generation in microbial reverse-electrodialysis electrolysis cells using a heat-regenerated salt solution, *Environ. Sci. Technol.*, 46 (2012) 5240-5246.
[47] X. Luo, et al., Methane production in microbial reverse-electrodialysis methanogenesis cells (MRMCs) using thermolytic solutions, *Environ. Sci. Technol.*, 48 (2014) 8911-8918.
[48] M.C. Hatzell, I. Ivanov, R. D. Cusick, X. Zhu, B.E. Logan, Comparison of hydrogen production and electrical power generation for energy capture in closed-loop ammonium bicarbonate reverse electrodialysis systems, *Phys. Chem. Chem. Phys.*, (2014).
[49] F. Mani, M. Peruzzini, P. Stoppioni, CO2 absorption by aqueous NH3 solutions: Speciation of ammonium carbamate, bicarbonate and carbonate by a 13C NMR study, *Green Chem.*, 8 (2006) 995-1000.
[50] H.-W. Kim, J.-Y. Nam, H.-S. Shin, Ammonia inhibition and microbial adaptation in continuous single-chamber microbial fuel cells, *J. Power Sources*, 196 (2011) 6210-6213.
[51] K.H. Yeon, J.H. Seong, S. Rengaraj, S.-H. Moon, Electrochemical characterization of ion-exchange resin beds and removal of cobalt by electrodeionization for high purity water production, *Separation Sci. and Technol.*, 38 (2003) 443-462.
[52] W.S. Miller, C.J. Castagna, A.W. Pieper, Understanding ion-exchange resins for water treatment systems, in: Plant Engineering, GE Water & Process Technologies, 2009.
[53] F.G. Helfferich, Ion exchange, McGraw-Hill, 1962.
[54] Conductivity temperature compensation, Thermo Fisher Scientific, thermoscientific.com/waterlibrary, 2011, pp. 2.
[55] A.H. Galama, et al., Membrane resistance: The effect of salinity gradients over a cation exchange membrane, *J. Mem. Sci.*, 467 (2014) 279-291.
[56] G.M. Geise, A.J. Curtis, M.C. Hatzell, M.A. Hickner, B.E. Logan, Salt concentration differences alter membrane resistance in reverse electrodialysis stacks, *Environ. Sci. Technol. Lett.*, 1 (2013) 36-39.
[57] Dowex resins technical information bulletin, Sigma-Aldrich, Sigma-Aldrich, 2014.
[58] Dow ion exchange resins - Void volume, The Dow Chemical Company, Dow Answer Center, 2014.
[59] G.M. Geise, M.A. Hickner, B.E. Logan, Ammonium bicarbonate transport in anion exchange membranes for salinity gradient energy, *ACS Macro Lett.*, 2 (2013) 814-817.
[60] D.A. Vermaas, M. Saakes, K. Nijmeijer, Doubled power density from salinity gradients at reduced intermembrane distances, *Environ. Sci. Technol.*, 45 (2011) 7089-7095.
[61] Ion exchange resins, Dow Water & Process Solutions, http://www.dowwaterandprocess.com/en/products/ion_exchange_resins, 2013.
[62] N. Wen, M.H. Brooker, Ammonium carbonate, ammonium bicarbonate, and ammonium carbamate equilibria: A Raman study, *J. of Phys. Chem.*, 99 (1995) 359-368.

[63] G.S. Jadhav, M.M. Ghangrekar, Performance of microbial fuel cell subjected to variation in pH, temperature, external load and substrate concentration, *Bioresour. Technol.*, 100 (2009) 717-723.
[64] Dowex fine mesh spherical ion exchange resins, Form No. 177-01509-904, Dow Water Solutions, msdssearch.dow.com, pp. 9.

APPENDIX A: NOMENCLATURE

MFC	Microbial fuel cell
OCV	Open circuit voltage
SGE	Salinity gradient energy
PRO	Pressure-retarded osmosis
RED	Reverse electro-dialysis
AEM	Anion exchange membrane
CEM	Cation exchange membrane
AmB	Ammonium bicarbonate, NH_4HCO_3
SR	Salinity ratio
MREC	Microbial reverse-electrodialysis cell
MRCC	Microbial reverse-electrodialysis chemical-production cell
TAN	Total ammonia nitrogen, mg/L
IEC	Ion exchange capacity, meq/L
MDC	Microbial desalination cell
MRMC	Microbial reverse-electrodialysis methanogenesis cell
$\boldsymbol{R_{ohmic}}$	Ohmic resistance, Ω
$\boldsymbol{R_{\Delta C}}$	Concentration layer resistance, Ω
$\boldsymbol{R_{BL}}$	Boundary layer resistance, Ω
$\boldsymbol{E_{OCV}}$	Open circuit voltage, V
$\boldsymbol{P_{net}}$	Net power, W/m^2
$\boldsymbol{j}$	Current density, A/m^2
$\boldsymbol{P_{pump}}$	Pumping power, W/m^2
$\boldsymbol{N_m}$	Number of membranes
$\boldsymbol{R}$	Resistance, Ω
$\boldsymbol{V}$	Voltage, V
$\boldsymbol{I}$	Current, A
$\boldsymbol{\rho}$	Solution resistivity, cm/mS
$\boldsymbol{\sigma}$	Solution conductivity, mS/cm
$\boldsymbol{\emptyset_{resin}}$	Volume fraction resin